Physics

Electricity & Magnetism fields

Okayama University   *Year* 2003

3-D finite element analysis of current distribution in HTS power cable taking account of E-J power law characteristic

Daisuke Miyagi*   Tomohiro Wakatsuki†   Norio Takahashi‡

Shinji Torii**   Kiyotaka Ueda††

*Okayama University
†Okayama University
‡Okayama University
**Central Research Institute of Electric Power Industry
††Superconductive Generation Equipment and Materials

3-D Finite Element Analysis of Current Distribution in HTS Power Cable Taking Account of E-J Power Law Characteristic

Daisuke Miyagi, Tomohiro Wakatsuki, Norio Takahashi, *Fellow, IEEE*, Shinji Torii, and Kiyotaka Ueda

Abstract—A method for analyzing the current distribution in high-T_c superconducting (HTS) power cable is examined by the aid of the novel use of anisotropic conductivity and three-dimensional finite element method in consideration of the E-J power law characteristic. The detailed current distribution in the cable is illustrated and the shielding effect of HTS shield is also examined.

Index Terms—E-J power law characteristics, HTS power cable, HTS shield, three-dimensional finite element analysis.

I. INTRODUCTION

CONTROLLING the current distribution in a multilayer superconducting cable uniformly is important in order to realize a compact and large capacity high-T_c superconducting (HTS) power cable [1]. The phenomenon of current imbalance should be exactly investigated by analyzing, for example, the effect of twist pitch, etc., on flux and current distributions to design an efficient cable. In the analysis of HTS cable, the critical state model [2] cannot be applicable. Then, the E-J characteristic should be taken into account in order to analyze the current distribution of a HTS cable accurately. However, reports of such analysis are few [3]. This is mainly because the three-dimensional (3-D) analysis of current distribution in a multilayer superconducting cable consisting of superconducting tapes spirally wound on a former is complicated.

In this paper, 3-D finite element analysis taking account of the nonlinear E-J power law characteristic is carried out by modeling such spirally wound superconducting tapes as conductors having an anisotropic conductivity [4], [5]. Furthermore, we calculated a model of HTS power cable composed of one-layer HTS conductor and one-layer HTS shield with twist. The effect of the n value and twist pitch on the current distribution is illustrated and the shielding effect of HTS shield is discussed.
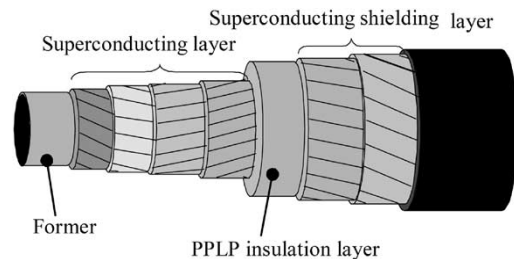
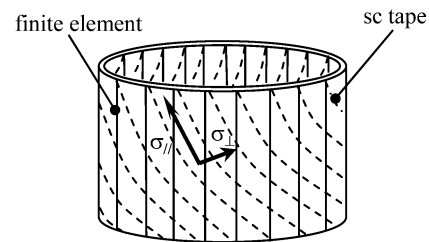Fig. 1. Structure of typical HTS cable composed of multilayered conductors.

Fig. 2. Modeling of cable conductors with anisotropy of conductivity.

II. METHOD OF ANALYSIS

A. Modeling of Cable Structure

An HTS cable should consist of multilayered conductors to increase its current loading. The structure of typical HTS cable is shown in Fig. 1. When there are many layers of superconductor in a superconducting cable, it is difficult to analyze magnetic fields in the cable using the conventional 3-D finite element method, because the number of finite elements increases greatly. If the cable is treated as a macroscopic one having anisotropic conductivity as shown in Fig. 2, the calculation can be carried out within an acceptable memory requirement and CPU time. Moreover, since it is not necessary to generate a mesh even if the twist pitch is changed, the optimal twist pitch can be easily examined.

The conductivity $\sigma_{//}$ parallel to the superconducting tape depends on the E-J power law characteristic. The conductivity $\sigma_\perp$ perpendicular to the superconducting tape is assumed by

$$\sigma_\perp = \frac{\sigma_{//}\sigma_m}{\lambda\sigma_m - (1-\lambda)\sigma_{//}} \qquad (1)$$

where σ_m is the conductivity of the silver sheath and λ is the volume fraction of superconductor in the HTS layer. The conductivity σ_m of silver sheath is 3.45×10^8 S/m (at 77 K) and the volume fraction λ is assumed as equal to 0.6.
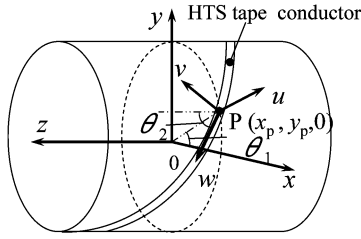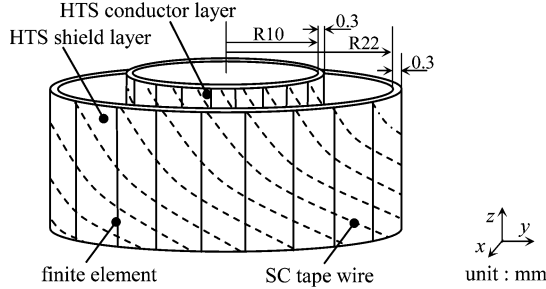
Fig. 3. Local coordinates.

Fig. 4. Analytical model of HTS power cable composed of one-layer HTS conductor and one-layer HTS shield.

TABLE I
SPECIFICATION OF FINITE ELEMENT MESH

	Without shield	With shield
Number of divisions in radial direction	176	285
Number of divisions in circumferential direction	2	2
Number of elements	351	569
Number of nodes	1058	1712

TABLE II
CASES OF CALCULATIONS FOR HTS POWER CABLE

Cases of calculation	i	ii	iii	iv	v	vi
Twist pitch of conductor (mm)	∞	300	∞	300	300	300
Twist pitch of shield (mm)	-	-	-	-	∞	300
n value	12	12	6	6	12	12
Direction of twist	-	s	-	s	ss	ss

ss : the same twist direction s of shield layer and conductor layer.

The conductivity of the anisotropic conductor is a tensor, of which the off-diagonal elements are all zero. The current density J_u, J_v, and J_w in the u-, v-, and w-directions defined along the superconducting tape as shown in Fig. 3 can be written using each component E_u, E_v and E_w of electric field strength E and $\sigma_\perp$ and $\sigma_{//}$ as follows [5]:

$$\begin{Bmatrix} J_u \\ J_v \\ J_w \end{Bmatrix} = \begin{bmatrix} \sigma_\perp & 0 & 0 \\ 0 & \sigma_\perp & 0 \\ 0 & 0 & \sigma_{//} \end{bmatrix} \begin{Bmatrix} E_u \\ E_v \\ E_w \end{Bmatrix}. \quad (2)$$

The relationship between J_x, J_y, and J_z and E_x, E_y, and E_z can be obtained as follows [5]:

$$\begin{Bmatrix} J_x \\ J_y \\ J_z \end{Bmatrix} = [K] \begin{bmatrix} \sigma_\perp & 0 & 0 \\ 0 & \sigma_\perp & 0 \\ 0 & 0 & \sigma_{//} \end{bmatrix} [K]^{-1} \begin{Bmatrix} E_x \\ E_y \\ E_z \end{Bmatrix}$$
$$= \begin{bmatrix} \sigma_a & \sigma_b & \sigma_c \\ \sigma_d & \sigma_e & \sigma_f \\ \sigma_g & \sigma_h & \sigma_i \end{bmatrix} \begin{Bmatrix} E_x \\ E_y \\ E_z \end{Bmatrix} \quad (3)$$

where $[K]$ is the transformation matrix [5].

We assume two models of HTS power cable. One is HTS power cable composed of one-layer HTS conductor. The other is HTS power cable composed of one-layer HTS conductor and one-layer HTS shield. Both models have the same dimensions of conductor layer. The difference between the models is the existence of the HTS shield layer. Fig. 4 shows a model with the shield layer. Table I shows the number of elements of both models, etc. The thicknesses of the conductor layer and the shield layer are both equal to 0.3 mm. The inner diameters of the conductor layer and the shield layer are 20 and 44 mm, respectively. The critical current density J_c of a conductor layer and a shield layer are both equal to 4.0×10^7 A/m^2. The applied transport current is sinusoidal $(I_p \sin \omega t)$ and the frequency is 50 Hz. The peak value of transport current I_p is equal to $0.55 I_c$ (I_c being critical current). The twist pitch and n value were changed

and six kinds of calculations were performed. The six cases of calculations are listed in Table II.

The superconducting cable is treated as a conductor having large conductivity. The magnetic field is analyzed using the 3-D edge-based hexahedral finite element method (A-ϕ method, A being magnetic vector potential, ϕ being electric scalar potential). The convergence criterion of ICCG method is chosen as 10^{-9}.

B. Conductivity of Superconductor to be Used in Numerical Analysis

The infinite conductivity $\sigma_{//}$ of the superconductor cannot be treated in the numerical calculation. Then, one needs to determine a suitable value for the conductivity $\sigma_{//}$ in (2) for the numerical analysis. The superconducting property is given by the E-J characteristic represented with a power law as follows:

$$E = E_c \left(\frac{J}{J_c} \right)^n \quad (4)$$

where E_c is assumed as equal to 1×10^{-4} V/m. Then, the equivalent conductivity of superconductor $\sigma_{//}$ is derived as

$$\sigma_{//} = \frac{J}{E} = \frac{J_c^n}{E_c} J^{1-n}. \quad (5)$$

$\sigma_{//}$ is determined iteratively at each time step Δt ($=5 \times 10^{-4}$ s) until the final result is obtained. The conductivity $\sigma_{//}^{(k)}$ at the kth iteration is given by

$$\sigma_{//}^{(k)} = \sigma_{//}^{(k-1)} + \alpha \left(\sigma_{//}^* - \sigma_{//}^{(k-1)} \right) \quad (6)$$

where $\sigma_{//}^*$ is the conductivity calculated using (5). α is the under-relaxation factor ($\alpha = 0.1$). The iteration is stopped when $\sigma_{//}^* - \sigma_{//}^{(k-1)}$ becomes less than 0.01. To enhance the efficiency of calculation, the maximum value of $\sigma_{//}$ is limited to 1.0×10^{13} S/m and the minimum value of $\sigma_{//}$ is limited to the conductivity σ_m of the silver sheath. On average, 100 iterations
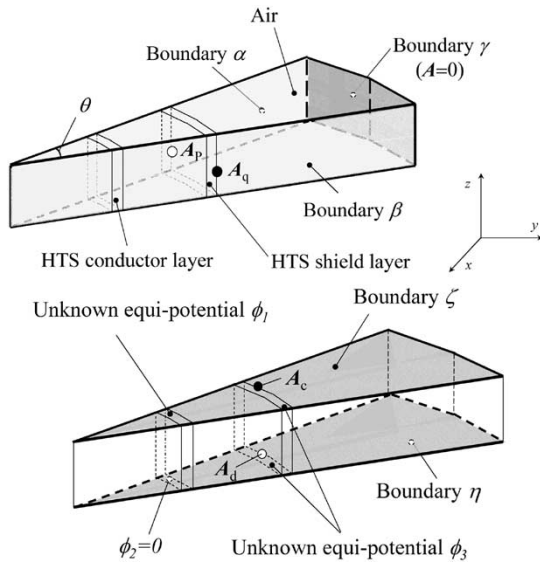
Fig. 5. Boundary condition and HTS cable model used for numerical calculation.

are necessary to obtain the current distribution considering the E-J characteristics.

C. Boundary Condition

Fig. 5 shows the boundary condition and the analysis region. Due to the symmetry of the analyzed model, let us assume that a point p on the boundary α (parallel to the z-axis) of the HTS conductor corresponds to a point q on the boundary β (parallel to the z-axis). The periodic boundary condition is given at the points p and q by assuming that the vector potential $\boldsymbol{A}_p$ at the point p is equal to $\boldsymbol{A}_q$ at the point q $(\boldsymbol{A}_p = \boldsymbol{A}_q)$. The analysis region is reduced to only $1/180$ of the whole region, taking the advantage of the periodic boundary. The Dirichlet boundary condition $(\boldsymbol{A} = 0)$ is given on the boundary γ (parallel to the x-y plane) of the air region. Let us assume that a point c on the boundary ζ of the HTS conductor corresponds to a point d on the boundary η (parallel to the x-y plane). The periodic boundary condition is given at the points c and d by assuming that the vector potential $\boldsymbol{A}_c$ at the point c is equal to $\boldsymbol{A}_d$ at the point d $(\boldsymbol{A}_c = \boldsymbol{A}_d)$.

The unknown equipotential condition of electric scalar potential ϕ_1 is given on the boundary ζ of the HTS conductor, and the equipotential $\phi_2 = 0$ is given on the boundary η. The electric scalar potential ϕ_3 on the boundary ζ of the HTS shield is equal to that on the boundary η, and this is treated as an unknown equipotential. (The electric scalar potential is defined only in the HTS conductor and HTS shield.)

III. NUMERICAL ANALYSIS AND DISCUSSION

A. HTS Power Cable Without Shield Layer

In order to investigate the influence of the twist pitch on a current distribution in a conductor layer, the calculation results of a case i and a case ii without a shield layer is compared. The current distribution of case i without twist pitch is shown in Fig. 6(a). The figure shows the current distributions in a conductor layer at $\omega t = -\pi/2$ (I_p is minus peak value) and at
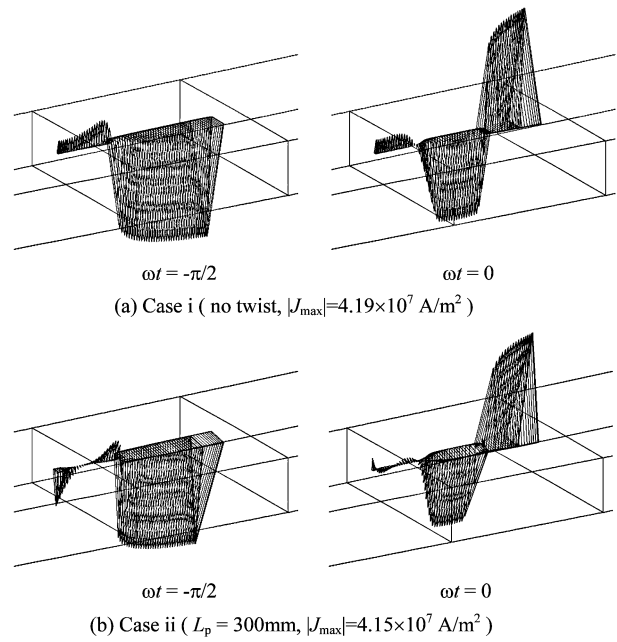

(a) Case i (no twist, $|J_{max}|$=4.19×10^7 A/m^2)

(b) Case ii (L_p = 300mm, $|J_{max}|$=4.15×10^7 A/m^2)

Fig. 6. AC current distributions in conductor layer (n value = 12).

(a) Case iii (no twist, $|J_{max}|$=4.43×10^7 A/m^2)

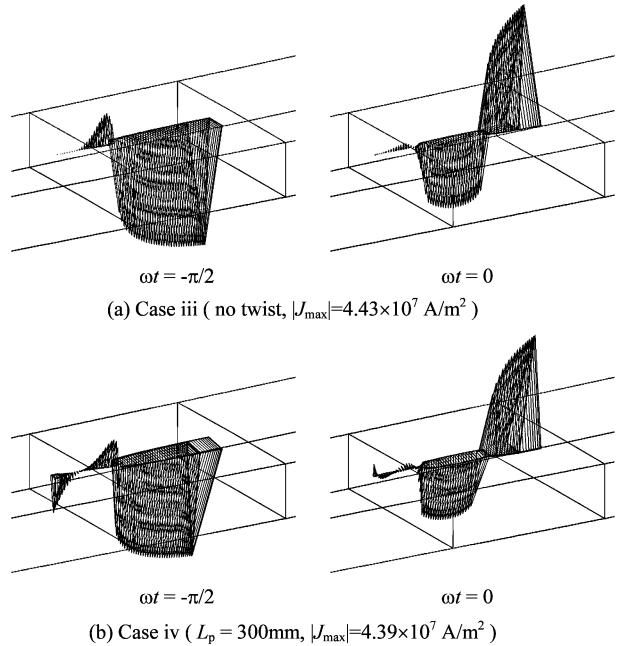(b) Case iv (L_p = 300mm, $|J_{max}|$=4.39×10^7 A/m^2)

Fig. 7. AC current distributions in conductor layer (n value = 6).

$\omega t = 0$ (I_p is zero). The calculation result of case ii with twist (twist pitch: $L_p = 300$ mm) is shown in Fig. 6(b). The n value of case i without twist and case ii with twist ($L_p = 300$ mm) are both equal to 12. Fig. 6 shows that the current diffuses into the conductor layer from the outer surface. Fig. 6(b) shows that current flows in the twist direction. The twist influences not only the direction of the current but also current distribution in a conductor layer.

The current distributions of case iii and iv are shown in Fig. 7. n value of case iii without twist and case iv with twist ($L_p = 300$ mm) are both equal to 6. Figs. 6 and 7 illustrate that the effect of the n value on the current distribution is small. The
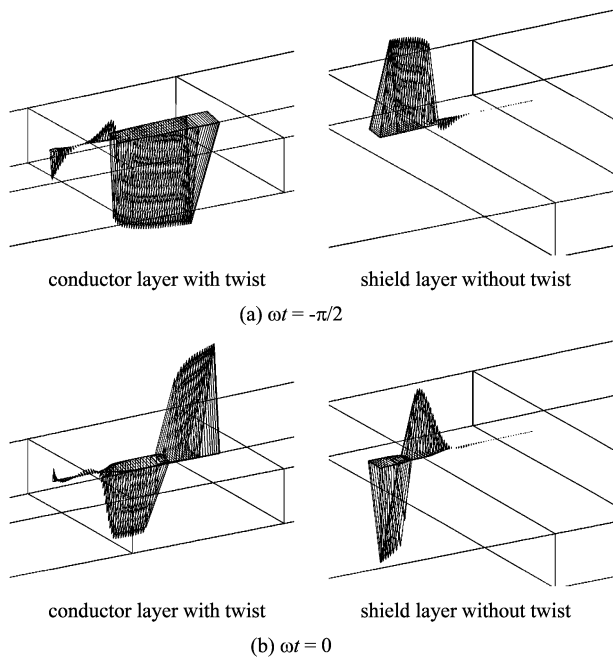
conductor layer with twist   shield layer without twist

(a) ωt = -π/2

conductor layer with twist   shield layer without twist

(b) ωt = 0

Fig. 8.   AC current distributions in a conductor layer and a shield layer (case *v*: conductor layer with twist $L_\mathrm{p} = 300$ mm, shield layer without twist, n value $= 12$).

conductor layer with twist   shield layer with twist

(a) ωt = -π/2

conductor layer with twist   shield layer with twist

(b) ωt = 0

Fig. 9.   AC current distributions in a conductor layer and a shield layer (case *vi*: conductor layer and shield layer are both with twist $L_\mathrm{p} = 300$ mm, n value $= 12$).

maximum value of current density $|J_\mathrm{max}|$ is slightly larger than J_c ($=4.0 \times 10^7$ A/m^2).

B. HTS Power Cable With Shield Layer

The current distribution in the HTS power cable model composed of a conductor layer and a shield layer is analyzed. Figs. 8 and 9 show current distributions of case *v* having shield layer without twist, and those of case *vi* having shield layer with twist ($L_\mathrm{p} = 300$ mm). The twist pitch of a conductor layer of case *v* and case *vi* are both equal to 300 mm. As shown in Fig. 8, the shield current has some circumferential component, although the shield layer is not twisted. Fig. 9(a) illustrates that the shield current flows along the twist direction. The above results suggest that the twist of the shield layer influences not only the current distribution of the shield layer but also the current distribution in the conductor layer. In order to develop a shield layer with an efficient shielding characteristic and low ac loss, it is necessary to investigate the distribution of shield current in detail in the future.

IV. SUMMARY

A method for analyzing the current distribution in high-T_c superconducting power cable is examined by the aid of novel use of anisotropic conductivity and 3-D finite element method
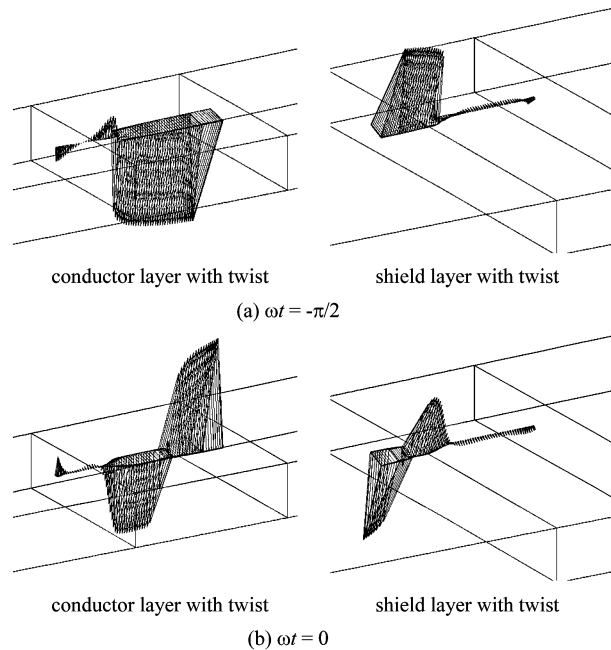
in consideration of E-J power law characteristics. The detailed current distribution in the cable is illustrated and the shielding effect of HTS shield is also examined. The effect of n value on the current distribution is small. The twist of the shield layer influences not only a current distribution of a shield layer but also a current distribution in a conductor layer. Since it is too difficult to measure current distributions in conductor and shield layers, the verification of our results by experiments is the subject of future work. The results of our analysis will give important information about the optimal design of HTS power cable.

REFERENCES

[1] S. Honjo, K. Matsuo, T. Miura, and Y. Takahashi, "High-T_c superconducting power cable development," *Physica C*, no. 357–360, pp. 1234–1240, 2001.
[2] M. Tsuchimoto and T. Honma, "Numerical evaluation of levitation force of HTSC flywheel," *IEEE Trans. Appl. Superconduct.*, vol. 4, pp. 211–215, Dec. 1994.
[3] N. Amemiya, K. Miyamoto, S. Murasawa, H. Mukai, and K. Ohmatsu, "Finite element analysis of AC loss in nontwisted Bi-2223 tape carrying AC transport current and/or exposed to DC or AC external magnetic field," *Physica C*, no. 310, pp. 30–35, 1998.
[4] W. J. Carr Jr., *AC Loss and Macroscopic Theory of Superconductors*.   New York: Gorden and Breach, 1983.
[5] N. Takahashi, T. Nakata, Y. Fujii, K. Muramatsu, M. Kitagawa, and J. Takehara, "3-D finite element analysis of coupling current in multifilamentary ac superconducting cable," *IEEE Trans. Magn.*, vol. 27, pp. 4061–4064, Sept. 1991.